The Infrared and Raman Spectra of Fullerene C 70 . DFT Calculations and Correlation with C 60

3 AUTHORS, INCLUDING:

Vincenzo Schettino
University of Florence
195 PUBLICATIONS **3,490** CITATIONS

SEE PROFILE

Gianni Cardini
University of Florence
171 PUBLICATIONS **2,372** CITATIONS

SEE PROFILE

The Infrared and Raman Spectra of Fullerene C$_{70}$. DFT Calculations and Correlation with C$_{60}$

Vincenzo Schettino,* Marco Pagliai, and Gianni Cardini

Laboratorio di Spettroscopia Molecolare, Dipartimento di Chimica, Università di Firenze, Via G. Capponi 9, 50121 Firenze, Italy, and European Laboratory for Nonlinear Spectroscopy (LENS), Largo E. Fermi 2, 50125 Florence, Italy

A DFT calculation of the vibrational frequencies of the infrared and Raman intensities of C$_{70}$ is reported using the B3-LYP exchange and correlation functional and the 6-31G* basis set. It's shown that a very good fit to the known infrared and Raman active modes is obtained. Using the calculated frequencies as a base guide, a full assignment of the C$_{70}$ vibrational frequncies is proposed. A correlation between the C$_{70}$ and the C$_{60}$ normal modes of vibrations is discussed.

I. Introduction

The vibrational spectra of fullerenes have attracted a considerable attention as a probe of structural and dynamic properties of these carbon clusters and of their solid-state properties.[1] However, a complete assignment of the normal modes poses considerable problems particularly because the high symmetry of the clusters makes many normal modes inactive in the infrared and Raman spectra.

In the case of the C$_{60}$ cluster a reliable assignment has been obtained taking advantage of the fact that in the crystal[2−6] and in substituted molecules[2] most of the normal modes become infrared or Raman active due to the reduced local symmetry. Using the experimental infrared and Raman spectra of the crystal and the ab initio DFT calculated normal frequencies[7] a complete assignment of the C$_{60}$ frequencies has been proposed by Schettino et al.[8] Later, a complete assignment of the C$_{60}$ mode has been rediscussed by Choi et al.[9] and by Menéndez and Page[10] on the same grounds. More recently Schettino et al.[11] have shown that a DFT B3LYP/6-31G* calculation of the vibrational frequencies of C$_{60}$ can grant an average misfit between the calculated and experimental frequencies of the active modes as low as ∼3.6 cm^{-1}. Therefore, the DFT calculation could be used with confidence to assign all the silent modes leading to an average difference between calculated and observed frequencies of ∼5 cm^{-1}.

To obtain a complete assignment of the C$_{70}$ cluster appears by far more complicated. In fact the number of normal modes is large (122 including 82 doubly degenerate modes) and some of these will have a very low infrared and Raman intensity. Also in this case one can expect most of the silent modes to become weakly active in the crystal at low temperature,[12,13] but it will not be straightforward to distinguish them from several of the free molecule active vibrations on intensity grounds. On the other hand there are semiempirical[14−21] and ab initio[22,23] calculations available of the normal frequencies of C$_{70}$. It appears, however, that the presently available calculations based on different levels of approximation differ substantially in

several cases. It is, therefore, not simple to decide which of the available calculations is the most reliable guide for the spectral assignment.

The purpose of the present paper is to rediscuss the vibrational spectra of fullerene C$_{70}$ using an approach based on three different but convergent points of view. First we report on a calculation of the vibrational frequencies and of the infrared and Raman intensities based on the DFT approach using the B3-LYP exchange-correlation functional and the 6-31G* basis set (the Raman intensities have been obtained with the smaller 3-21G basis set). This approach has been found to be quite reliable for C$_{60}$[11] and for other conjugated molecules[24−26] and can be taken with confidence as a basic guide for the vibrational assignment. As a matter of fact, the reliability of the DFT approach at the B3-LYP/6-31G* level to calculate the vibrational frequencies of C$_{70}$ has been demonstrated by Stratmann et al.,[27] but their analysis has been confined to the infrared active modes.

In addition two different types of symmetry arguments and correlation have been exploited, the first based on an attempt to correlate the C$_{70}$ frequencies with the known frequencies of C$_{60}$. The basis for this correlation is found in common subgroups of the I_h and D_{5h} symmetry groups of C$_{60}$ and C$_{70}$ molecules. A second symmetry correlation is carried out considering the C$_{70}$ cluster as a cyclic system under the C$_5$ subgroup of D_{5h} and classifying the C$_{70}$ vibrations in diagrams recalling the dispersion curves of a crystal.

A reasonable interpretation of the crystal phase infrared and Raman spectra can be obtained using the results of the DFT calculations and the possible symmetry considerations.

II. Computational Details and Experimental

Calculations of the vibrational frequencies of C$_{70}$ were carried using the density functional theory. According to Rauhut and Pulay[28] and to Scott and Radom[29] the use of the B3-LYP exchange-correlation functional in conjunction with the 6-31G* basis constitutes the best compromise between applicability to large molecules and computer resources. This approach has been applied with considerable success to C$_{60}$[11] and, with a single scaling factor of 0.98 on the calculated frequencies, has been shown to be able to reproduce the experimental frequencies with very good accuracy. The same approach has been extended to

* To whom correspondence should be addressed. E-mail: schettin@chim.unifi.it

1816 *J. Phys. Chem. A, Vol. 106, No. 9, 2002*

Schettino et al.
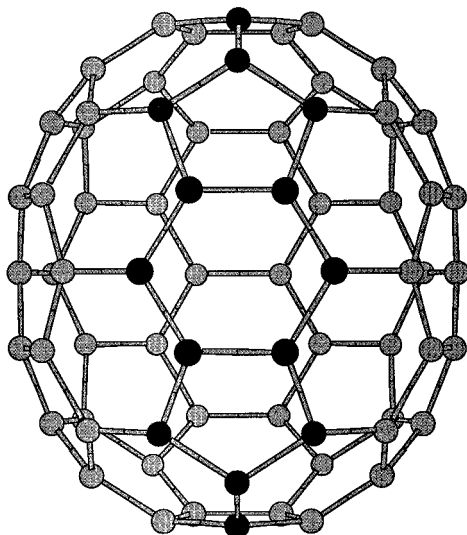
Figure 1. The C_{70} cluster: the 14 atom generating set according to the C_5 group is drawn in black.

the to C_{70} molecule. After a very tight optimization of the geometry, the vibrational frequencies have been calculated using the GAUSSIAN 98 rev A.7 suite of programs.[30] The calculated frequencies have been scaled uniformily by a factor 0.98, as already proposed by Stratmann et al.[27]

The infrared intensities have been calculated using the 6-31G* basis set while the Raman intensities could only be obtained with the 3-21G basis set. The vibrational frequencies and the infrared intensities have been calculated also for the $^{12}C_{59}{}^{13}C$ species, considering the five possible distinct positions of the ^{13}C isotope.

The infrared spectra of C_{70} films of various ticknesses have been measured at various temperatures using a Brucker IFS HR120 Fourier transform spectromer with a resolution of 0.5 cm^{-1}. The Raman spectra at room temperature have been performed with the FT Raman option of the Brucker interferometer. Commercial sample of C_{70} from Syncom have been used without further purification.

III. Symmetry Considerations

The free C_{70} cluster belongs to the D_{5h} symmetry group and the 204 normal vibrations classify as $12A_1' + 9A_2' + 21E_1' + 22E_2' + 9A_1'' + 10A_2'' + 19E_1'' + 20E_2''$. The E_1' and A_2'' modes are infrared active and the A_1', E_2' and E_1'' are Raman active. For the following discussion it may be helpful to recall that the ′ and ″ vibrations are symmetric and antisymmetric with respect to the equatorial symmetry plane, respectively. It is also recalled that the normal vibrations of C_{60} classify in the I_h symmetry group as $2A_g + 3T_{1g} + 4T_{2g} + 6G_g + 8H_g + A_u + 4T_{1u} + 5_{2u} + 6G_u + 7H_u$.

A direct correlation between two molecules with I_h and D_{5h} symmetries cannot be found since the latter is not a subgroup of the former. However, we notice, as it can be seen from Figure 1, that the C_{70} cluster can be viewed as formed by two semicircular caps of 30 carbon atoms, substantially identical to half the C_{60} cluster, separated by an equatorial belt of 10 atoms. As a working hypothesis it will be assumed that the vibrational modes of the equatorial belt (30 modes) are not coupled with those of the semispherical caps. The validity of this hypothesis will be checked a posteriori. Within this assumption we may try to correlate the vibrations of the semispherical caps of C_{70} with those of C_{60}.

TABLE 1: Correlation Diagrams of the I_h and D_{5h} Groups with Common Subgroups

I_h	D_5	D_{5h}	C_{5v}	I_h
A_g, A_u	A_1	A_1'	A_1	A_g
		A_1''		A_u
T_{1g}, T_{1u}	A_2	A_2'	A_2	T_{1g}
		A_2''		T_{2g}
T_{2g}, T_{2u}	E_1	E_1'	E_1	T_{1u}
		E_1''		T_{2u}
G_g, G_u	E_2	E_2'	E_2	G_g, G_u
		E_2''		H_g
H_g, H_u				H_u

**TABLE 2: Correspondence between the Vibrations of C_{60} in the I_h and D_{5h} Groups**

I_h	D_{5h}	I_h	D_{5h}
A_g	A_1'	T_{2u}	$A_2'' + E_2''$
A_u	A_1''	G_g	$E_1' + E_1''$
T_{1g}	$A_2' + E_1'$	G_u	$E_1'' + E_2''$
T_{2g}	$A_2' + E_2''$	H_g	$A_1' + E_1' + E_1''$
T_{1u}	$A_2'' + E_1'$	H_u	$A_1'' + E_1'' + E_2''$

TABLE 3: Correlation of the C_{70} Vibration in the D_{5h} with the C_{60} Type Vibrations in the I_h Group and with the Vibrations of the Equatorial Belt (Eq)

$$12A_1' \leftrightarrow 2A_g + 8H_g + 2Eq$$
$$9A_2' \leftrightarrow 3T_{1g} + 4T_{2g} + 2Eq$$
$$21E_1' \leftrightarrow 3T_{1g} + 6G_g + 8H_g + 4Eq$$
$$22E_2' \leftrightarrow 4T_{2g} + 6G_g + 8H_g + 4Eq$$
$$9A_1'' \leftrightarrow A_u + 7H_u + 1Eq$$
$$10A_2'' \leftrightarrow 4T_{1u} + 5T_{2u} + 1Eq$$
$$19E_1'' \leftrightarrow 4T_{1u} + 6G_u + 7H_u + 2Eq$$
$$20E_2'' \leftrightarrow 5T_{2u} + 6G_u + 7H_u + 2Eq$$

For this purpose we notice that I_h and D_{5h} have D_5 and C_{5v} as common subgroups and correlate the C_{60} and C_{70} vibrations through these common subgroups. The correlation diagrams are reported in Table 1. Through a single common subgroup, the correlation of the C_{60} and C_{70} vibrations is not unambiguous. However, if a double compatibility from Table 1 is required, it is readily found that the correlation is unique in several cases. Whenever an ambiguity remains we consider the character in the starting irriducible representation of the I_h group and require it to equal the character of the direct sum of the corresponding representations of the D_{5h} group. For instance, from Table 1 it is seen that the T_{1g} species correlates clearly with the A_2' species and with either the E_1' or E_1'' species. Comparing the characters for the E, C_5, C_2, σ_h, and C_5^2 operations the choice falls in the E_1'' species.

The results are summarized in Table 2 where it is shown how the C_{60} vibrations would transform under a D_{5h} symmetry. Alternatively, the table shows, for each vibration of the semispherical cap of C_{70}, from which mode of the C_{60} cluster can be considered to derive. The vibrational modes of the equatorial belt should be considered in addition and these classify as $2A_1' + 2A_2' + 4E_1' + 4E_2' + A_1'' + A_2'' + 2E_1'' + 2E_2''$. In conclusion the vibrations of C_{70} can be correlated with those of C_{60} as shown in Table 3 which is the reverse of Table 2 and where the vibrations of the equatorial belt are also displayed. It is clear from Table 2 that once the normal vibrational frequencies of C_{60} are known it should, by comparison, be easy to look in the infrared and Raman spectra for the location of the normal frequencies of C_{70}. This same type correlation between the C_{60} and C_{70} vibrations has been considered by Brockner and Menzel[31] who, however, did not give a symmetry justification for the correlation.

Fullerene C$_{70}$ Spectra

J. Phys. Chem. A, Vol. 106, No. 9, 2002 **1817**
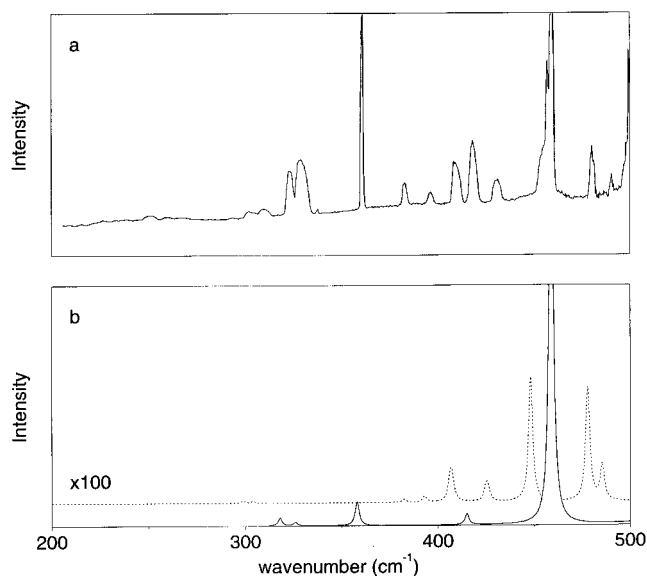
Figure 2. Far-infrared spectrum of C$_{70}$. a: Experimental. b: Calculated (Full line: infrared active fundamentals in ^{12}C$_{70}$. dotted lines: Silent modes in ^{13}C^{12}C$_{69}$.).
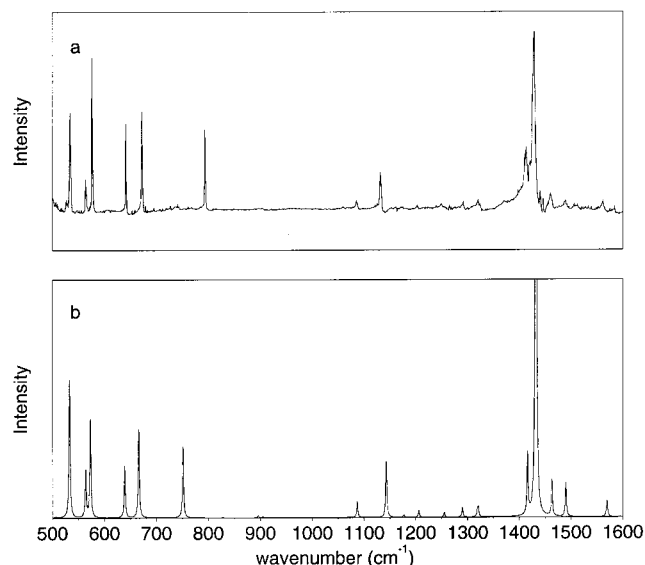
Figure 3. Infrared spectrum of C$_{70}$. a: Experimental. b: Calculated for ^{12}C$_{70}$.

From a different point of view, the C$_{70}$ normal vibrations can be classified considering the cyclic C$_5$ subgroup of D_{5h}. Using this subgroup the C$_{70}$ molecule can be viewed as originating from a set of 14 carbon atoms, shown in Figure 1, that are "translated" by the symmetry operations of the C$_5$ group. According to this approach the normal frequencies of the C$_{70}$ clusters can be viewed as giving rise to dispersion curves as it is customary in crystals under periodic boundary conditions, with the 14 carbon atoms generating set playing the role of the unit cell and with permissible values of the wavevector of 0, cos$2\pi/5$, cos$4\pi/5$, cos$6\pi/5$, and cos$8\pi/5$. As it is seen from the character table of the C$_5$ group, the normal frequencies with wavevectors cos$2\pi/5$, cos$8\pi/5$ and cos$4\pi/5$, and cos$6\pi/5$ are degenerate. Considering for convenience the vibrations that are symmetric and antisymmetric with respect to the equatorial plane we may construct two subsets of the dispersion curves arising from the vibrations (A$_1'$ + A$_2'$) → E$_{1a}'$ → E$_{2a}'$ → E$_{2b}'$ → E$_{1b}'$ and (A$_1''$ + A$_2''$) → E$_{1a}''$ → E$_{2a}''$ → E$_{2b}''$ → E$_{1b}''$. Since the set of the 14 generating carbon atoms has a local symmetry C$_{2v}$ the dispersion
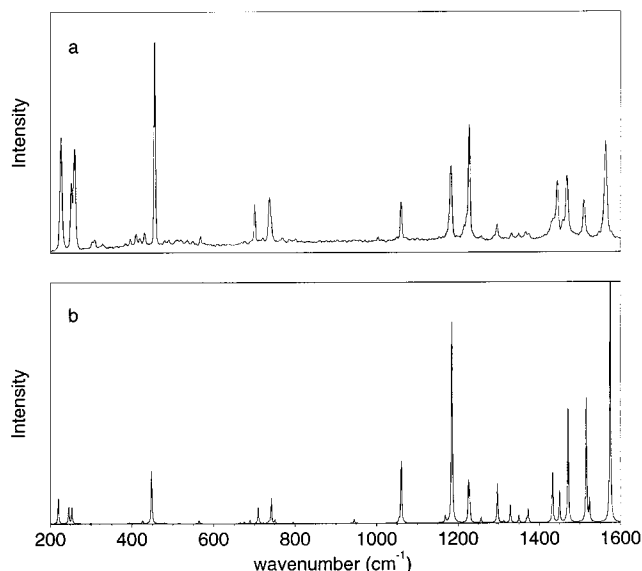
Figure 4. Raman spectrum of C$_{70}$. a: Experimental. b: Calculated for ^{12}C$_{70}$.

TABLE 4: Calculated and Observed Fundamental Vibrational Frequencies of C$_{70}$

A$_1'$		A$_2'$		A$_1''$		A$_2''$	
calcd	obs	calcd	obs	calcd	obs	calcd	obs
253	260	486	490	336	337	318	320
393	396	546	543	529	527	458	458
448	455	628	621	612	609	564	564
564	568	732		734		704	707
702	697	745	750	780	785	896	901
709	701	936	938	892	892	1143	1133
1061	1060	1215	1215	1241	1241	1206	1203
1185	1182	1339	1342	1348		1321	1320
1229	1222	1451	1442	1559	1550	1463	1460
1450	1459					1568	1557
1472	1468						
1575	1576						

E$_1'$		E$_2'$		E$_1''$		E$_2''$	
calcd	obs	calcd	obs	calcd	obs	calcd	obs
326	328	220	225	245	250	304	309
358	361	299	303	408	410	383	382
415	418	426	430	479	480	407	412
507	509	503	505	515	520	515	522
533	534	533	535	546	548	556	557
573	578	665	668	675	675	633	
639	642	689	688	714	712	701	690
666	674	722	721	735	733	717	709
730	728	735	738	741	741	728	726
751	795	741	743	795	800	782	790
828	835	750	768	1055	1050	920	922
905	904	767	760	1169	1172	1075	1070
1087	1087	945	948	1226	1227	1156	1152
1177	1176	1059	1055	1297	1227	1258	1261
1255	1251	1187	1196	1313	1311	1316	1316
1290	1291	1257	1258	1369	1367	1328	1338
1319	1321	1329	1332	1433	1367	1399	1400
1416	1414	1350	1349	1433	1445	1455	1455
1432	1430	1373	1374	1516	1511	1517	1528
1490	1489	1501	1500	1574	1545	1573	1565
1570	1563	1524	1520				
		1574	1580				

curves can actually be classified into 4 subsets. The advantage of such a classification is that the multitude of normal frequencies is at least distinguished into subsets of five frequencies differing only by the phase factor of the atomic motions in the five molecular sectors.

TABLE 5: Experimental and Calculated Frequencies of C_{70}, Vibrational Assignment, and Correlation with the C_{60} Vibrational Mode

| Raman | | | | | infrared | | INS | calcd | symmetry | |
this work	ref 35	ref 36	ref 37	ref 38	this work	ref 36	ref 39	this work	C_{70}	C_{60}
225	226	225	231	224	227		229	220	E_2'	$H_g(1)$
			233[b]	229[b]						
250	251	252	252	252	251		252	245	E_1''	$H_g(1)$
			253[b]							
260	259	258	267	260	260		266	253	A_1'	$H_g(1)$
	266[b]				267[b]					
					294					
303	302	303	303		302		305	299	E_2'	E_q[a]
309	309		310		310		311	304	E_2''	$T_{2u}(1)$
320	323				324			318	A_2''	$T_{2u}(1)$
327	329	328			329			326	E_1'	$G_u(1)$
337		338	335		338		335	336	A_1''	$H_u(1)$
			338[b]							
362	361	362	362		363		366	358	E_1'	$H_u(1)$
382	383	383			384		386	383	E_2''	$G_u(1)$
396	396	397		400	396			393	A_1'	$H_g(2)$
410	410	409	408	413	409		402	408	E_1''	$H_g(2)$
			410[b]							
					412			407	E_2''	$H_u(1)$
419	419	419	418		419	418	418	415	E_1'	E_q
			420[b]							
430	430	431	434	436	431	430	438	426	E_2'	$H_g(2)$
455	455	454	458		454			448	A_1'	$A_g(1)$
					457	458	461	458	A_2''	$T_{1u}(1)$
					459[b]					
470					461					
480	480		479		479			479	E_1''	$G_g(1)$
490	490		491		490		494	486	A_2'	E_q
505	506	507	506					503	E_2'	$G_g(1)$
			507[b]							
510	511	513				510		507	E_1'	$H_u(2)$
520	521	519	520	521			519	515	E_1''	E_q
		522	523					515	E_2''	$H_u(2)$
					527			529	A_1''	$H_u(2)$
535	536	537	537		533	530		533	E_1''	$T_{2g}(1)$
					535	534	541	533	E_1'	$T_{1u}(1)$
						536[b]				
					543			546	A_2'	$T_{2g}(1)$
548	549				549			546	E_1''	$T_{1g}(2)$
553					557			556	E_2''	E_q
					565	566		564	A_2''	$T_{1u}(2)$
568	568	569	569	572	568			564	A_1'	E_q
573	578		578		578		582	573	E_1'	$T_{1u}(2)$
586										
609						606		612	A_1''	$H_u(3)$
621						618		629	A_2'	$T_{1g}(1)$
			643		642	643		639	E_1'	$H_u(3)$
			661							
668		669	670		669		653	665	E_2'	$G_g(2)$
					672					
675	676	675	674					675	E_1''	$G_g(2)$
					675	676		666	E_1'	$H_u(4)$
			677		677					
			680							
			683							
688	688					688	682	689	E_2'	$H_g(3)$
	690							701	E_2''	$T_{2u}(2)$
695	695	697	697		696	698		702	A_1'	$H_g(3)$
701	701	702	703		702			709	A_1'	$H_g(4)$
		707			707	708		704	A_2''	$T_{2u}(2)$
					709			717	E_2''	$H_u(4)$

Fullerene C$_{70}$ Spectra

J. Phys. Chem. A, Vol. 106, No. 9, 2002 **1819**

TABLE 5: (Continued)

Raman					infrared		INS	calcd	symmetry	
this work	ref 35	ref 36	ref 37	ref 38	this work	ref 36	ref 39	this work	C$_{70}$	C$_{60}$
712	713	714			713	712		714	E$_1''$	H$_g$(3)
						716^b				
718	721	721			721		720	722	E$_2'$	T$_{2g}$(2)
					726			728	E$_2''$	G$_u$(2)
			729		728	728		730	E$_1'$	G$_u$(2)
			733					735	E$_1''$	G$_g$(3)
737	736	738	738		738	738		735	E$_2'$	G$_g$(3)
			740		742			741	E$_1''$	H$_g$(4)
		743	743		745	744		741	E$_2'$	H$_g$(4)
750					752		751	745	A$_2'$	T$_{2g}$(3)
					758					
760					760			767	E$_2'$	T$_{2g}$(3)
	762	763			762					
					765					
768	768	768	768		768	768		750	E$_2'$	Eq
773					774	773	778			
784	786	785	785		785	785		780	A$_1''$	Eq
			790		790	790		782	E$_2''$	G$_u$(3)
		795	795		795	796		751	E$_1'$	Eq
800	801		800		800			795	E$_1''$	T$_{1g}$(2)
					835	835	850	828	E$_1'$	G$_u$(3)
					892	889		892	A$_1''$	A$_u$(1)
					898	898	899	896	A$_2''$	T$_{2u}$(3)
		904				904		905	E$_1'$	G$_u$(4)
					922	923		920	E$_2''$	T$_{2u}$(3)
					938	938		936	A$_2'$	T$_{1g}$(2)
	946	948	948		947	948	956	945	E$_2'$	Eq
1048		1050		1053	1050			1055	E$_1''$	G$_g$(4)
					1055			1059	E$_2'$	G$_g$(4)
1060	1060	1061	1061	1063	1062	1060		1061	A$_1'$	H$_g$(5)
1070	1071		1069		1071	1072		1075	E$_2''$	G$_u$(4)
1086	1086	1087	1089		1087	1088	1080	1087	E$_1'$	Eq
1098	1099									
					1105	1105				
					1120					
					1127	1127				
					1134	1136		1143	A$_2''$	T$_{1u}$(3)
1152	1152				1150	1150		1156	E$_2''$	T$_{2u}$(4)
	1156^b				1154					
1162	1163	1164		1167	1163	1162		1177	E$_1'$	T$_{1u}$(3)
1172	1172	1174	1176		1176	1176		1169	E$_1''$	H$_g$(5)
1182	1182	1184	1187	1187				1185	A$_1'$	Eq
1196			1189		1196	1196		1187	E$_2'$	H$_g$(5)
1205					1205	1208	1202	1206	A$_2''$	T$_{2u}$(4)
1215	1215	1218	1217		1218	1217		1215	A$_2'$	T$_{1g}$(3)
1222	1221	1224	1223			1226		1229	A$_1'$	H$_g$(6)
1227	1227	1229	1229	1232		1231		1226	E$_1''$	H$_g$(6)
1240	1241				1241	1241		1241	A$_1''$	H$_u$(5)
1245	1248				1251	1246		1255	E$_1'$	H$_u$(5)
1258	1257	1258	1258	1259	1258	1252		1257	E$_2'$	H$_g$(6)
						1258				
	1267		1261					1258	E$_2''$	H$_u$(5)
					1277	1275				
1285	1286				1284	1285				
	1296				1292	1292	1286	1290	E$_1'$	Eq
1296		1298	1297	1301	1302			1297	E$_1''$	T$_{1g}$(3)
1310		1313	1311	1316	1311	1310		1313	E$_1''$	G$_g$(5)
1316					1316	1314		1316	E$_2''$	G$_u$(5)
		1321	1322		1321	1320		1319	E$_1'$	G$_u$(5)
					1325			1321	A$_2''$	Eq
1332	1331	1335	1335	1335		1336		1329	E$_2'$	G$_g$(5)
			1338					1328	E$_2''$	H$_u$(6)

TABLE 5: (Continued)

Raman					infrared		INS	calcd	symmetry	
this work	ref 35	ref 36	ref 37	ref 38	this work	ref 36	ref 39	this work	C_{70}	C_{60}
1342					1343			1339	A'_2	$T_{2g}(4)$
1349	1349		1351		1352	1350	1355	1350	E'_2	$T_{2g}(4)$
						1354^b				
1367	1366	1368			1362	1364		1367	E''_1	Eq
1374	1374	1376	1377	1371	1370	1370		1373	E'_2	$H_g(7)$
						1376^b				
					1383	1384				
					1390	1389				
1400					1400	1405		1399	E''_2	Eq
1410	1413	1414			1416	1414		1416	E'_1	$H_u(6)$
	1424				1423	1426				
1430	1430	1432	1432		1428	1430		1432	E'_1	$T_{1u}(4)$
					1430^b					
					1432^b					
1435	1435	1436								
				1439	1439	1438				
				1443^b	1442^b	1442^b		1451	A'_2	Eq
1445	1445	1448	1447	1449	1447	1448		1433	E''_1	$H_g(7)$
						1452				
					1455	1456		1455	E''_2	$G_u(6)$
1460	1458	1460	1459	1463	1458			1450	A'_1	$H_g(7)$
					1462	1460		1463	A''_2	$T_{1u}(4)$
1468	1467	1467	1471	1471	1471	1466		1472	A'_1	$A_g(2)$
		1472^b				1472^b				
1480	1479				1479	1478				
	1484				1490	1488		1490	E'_1	$G_u(6)$
		1496			1493					
1500								1501	E'_2	$G_g(6)$
					1508	1506				
						1510				
1511	1511	1513	1514	1515	1514	1514		1516	E''_1	$G_g(6)$
1520					1519			1524	E'_2	Eq
1528					1529	1528		1517	E''_2	$T_{2u}(5)$
1533					1535	1534				
1545	1546		1546					1574	E''_1	$H_g(8)$
1550					1552	1552		1559	A''_1	$H_u(7)$
	1558	1557			1557	1557		1568	A''_2	$T_{2u}(5)$
					1563	1562		1570	E'_1	$H_u(7)$
1564	1565	1566	1564					1573	E''_2	$H_u(7)$
	1568									
1576			1578					1574	A'_1	$H_g(8)$
1580					1581	1583		1575	E'_2	$H_g(8)$
					1585					

a Eq = equatorial. *b* Component of a crystal splitting.

IV. Results and Discussion

The infrared spectrum of C_{70} below 400 cm^{-1} has been reported by von Czarnowski and Meiwes-Broer[32] but not in sufficient details for the purpose of a complete assignment of all the vibrational modes. In Figure 2 the low-frequency portion of the infrared spectrum of C_{70} at 8 K is shown and compared with the calculated spectrum. It can be seen that the agreement between calculations and experiments is excellent and this allows a straightforward identification of the low-frequency infrared fundamentals. It can be seen from the figure that beside the infrared fundamentals other weak bands appear in the spectrum, very much like it has been reported for the C_{60} crystals. In the low-frequency region of the spectrum these peaks must evidently be interpreted as Raman or silent modes that are made active by symmetry reduction in crystal or by the presence in the sample of a mixture of $^{12}C_{70}$ and $^{12}C_{69}^{13}C$ species

in the approximate ratio 10:7. As a matter of fact in the C_{60} crystal it has been shown by Procacci and Berne[33] and Procacci[34] that the intermolecular interactions are very effective in activating silent modes in the infrared spectrum. In a previous work on C_{60}[11] we have calculated the infrared spectrum of the $^{12}C_{59}^{13}C$ isotopomer showing that most the silent modes acquire a small but not negligible infrared intensity, in particular in the vicinity of the infrared fundamentals, where the mode mixing and the intensity transfer induced by the symmetry reduction is particularly effective. The same type of calculation has been carried also for the C_{70} cluster obtaining similar results with the additional complication that there are several non equivalent positions for the isotope substitution. The calculated spectrum of $^{12}C_{69}^{13}C$ isotopomer is also shown in Figure 2.

In Figure 3 a portion of the spectrum in the middle infrared region is compared with calculations. It can be seen that the fit

TABLE 6: Correlation between the Calculated C$_{70}$ and C$_{60}$ Vibrational Frequencies (in cm^{-1})

C$_{60}$ symmetry	ν	A_1'	A_2'	E_1'	E_2''
A_g	487	448			
	1473	1472			
T_{1g}	561		629		546
	824		936		795
	1277		1215		1297
T_{2g}	555		546	533	
	723		732	722	
	789		745	767	
	1345		1399	1350	
G_g	480			503	479
	565			665	675
	741			735	735
	1073			1059	1055
	1308			1329	1313
	1507			1501	1516
H_g	261	253		220	245
	429	393		426	408
	705	702		689	714
	772	709		741	1169
	1105	1061		1187	1226
	1251	1229		1257	1257
	1426	1450		1373	1433
	1585	1575		1574	1574
equat.		564	486	451	299
modes		1185	1451	751	750
				1087	945
				1290	1524

C$_{60}$ symmetry	ν	A_1''	A_2''	E_1''	E_2''
A_u	947		892		
T_{1u}	527	507		458	
	577	573		564	
	1190	1177		1143	
	1431	1432		1463	
T_{2u}	336			318	304
	709			704	701
	958			896	920
	1177			1206	1156
	1535			1568	1517
G_u	351	326			383
	737	730			728
	751	828			782
	963	905			1075
	1308	1319			1316
	1435	1490			1455
H_u	400	358	336		407
	530	507	529		515
	666	639	612		633
	728	666	734		717
	1220	1255	1241		1258
	1343	1416	1348		1328
	1576	1570	1559		1573
equat.		780	1321	515	556
modes				1367	1399

is excellent concerning both peak positions and intensities. On these grounds one can easily proceed to the identification of all the infrared active modes, on the basis primarily of the comparison, in the various spectral regions, of the relative infrared intensities. The only significant misfit concerns the E_1' mode calculated at 751 cm^{-1} and observed at 795 cm^{-1}. This misfit was already noted and discussed by Stratmann et al.[27] We mention that the frequency of this mode is the most sensitive to the basis set and increases considerably changing from the 3-21G to the 6-31G* basis. We shall return to the nature of this mode later. The assignment of the infrared modes of C$_{70}$ is summarized in Table 4, and coincides with that proposed by Stratmann et al.[27] except for the highest frequencies E_1' mode. However, the present assignment of the infrared modes is complete. The average difference between calculated and observed frequencies in the A_2'' and E_1' species is 3.2 and 5.9 cm^{-1}, respectively. It can be noted in the E_1' species ∼30% of the misfit should be attributed to the mode calculated at 751 cm^{-1} and discussed above. The general agreement is quite satisfactory and comparable to that found in C$_{60}$, confirming that for this kind of systems the DFT approach at the B3-LYP/6-31G* level can be used with confidence.

It is possible to proceed in the same way to analyze the Raman spectrum. In Figure 4 the calculated and experimental spectra are compared. In the present case some caution is necessary in considering the Raman intensities since these depend appreciably on the exciting line wavelength[35−38] and the calculations refer to fully out of resonance excitation conditions. In addition calculations of the Raman intensities could only be carried with the 3-21G basis set. In any case it can be seen from the figure that the agreement between calculations and experiments is surprisingly good, although not quantitative, also for the Raman spectrum. Also in the Raman spectrum of the crystal several additional features appear[35−38] that can be associated with weakly activated silent or infrared modes. Therefore, using as a guide the calculated Raman frequencies and relative Raman intensities one easily obtains

the assignment summarized in Table 4. It can be seen that the average discrepancy between observed and calculated frequencies is 4.9, 4.3, and 4 cm^{-1} for the A_1', E_1'', and E_2' species, respectively.

Encouraged by the results obtained for the infrared and Raman active species, the calculated frequencies have be used with confidence to identify among the weak infrared and Raman peaks the remaining silent modes. The results of such an attempt to complete the assignment for C$_{70}$ are collected in Table 4 from which it can be seen that only three modes remain unassigned, most likely because they are coincident with active modes. For the A_2', A_1'', and E_2'' symmetry species the average difference between calculated and observed frequencies comes out to be 4.1, 3.3, and 4.3 cm^{-1}, comparable to the values obtained for the active species.

The available experimental frequencies used to obtain the assignment reported in Table 4 and resulting from Raman[35−38] and infrared[36] spectroscopies, inelastic neutron scattering[39] experiments, and from the present work are collected in Table 5 with the values of the calculated frequencies and the assignment to the symmetry species of the molecular group. In the last column of the table the symmetry of the C$_{60}$ normal modes from which, according to the symmetry correlation discussed in the previous section, the C$_{70}$ normal mode can be considered to derive is reported. The correlation of the C$_{60}$ and C$_{70}$ vibrations is illustrated in Table 6 where the modes that can be considered to be mainly localized in the equatorial belt are also displayed. By visual inspection of the form of the normal modes and of the associated atomic displacements by molecular graphics programs, the "equatorial" normal vibrations are in most cases easily identified. Looking at the normal vibrations more quantitatively, it turns out that in the modes classified as equatorial the average displacement of the atoms in the equatorial belt is larger than for the others. No such degree of localization can be found for the other sets of atoms in the cluster. Such a localization of the normal modes is at first sight surprising, particularly by comparison with the C$_{60}$ case where
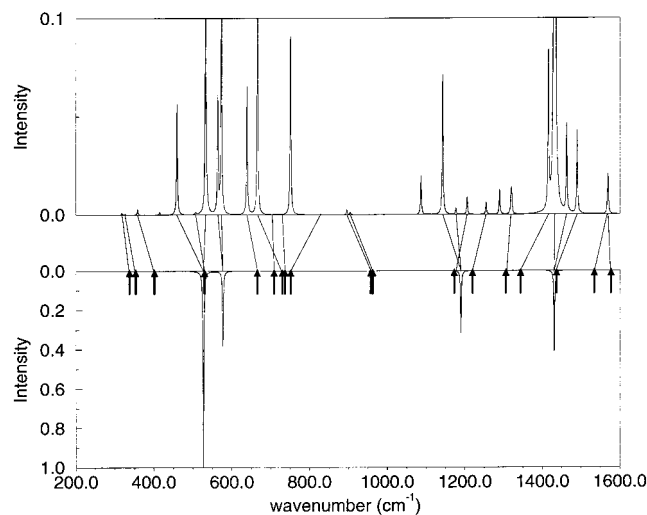
Figure 5. Correlation of the calculated infrared spectra of C_{70} (higher part) and C_{60} (lower part). The arrows indicate the position of silent modes in C_{60}.
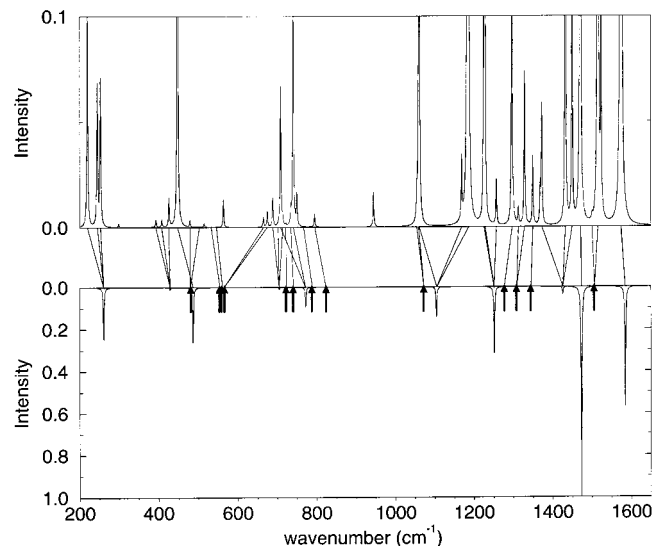

Figure 6. Correlation of the calculated infrared spectra of C_{70} (higher part) and C_{60} (lower part). The arrows indicate the position of silent modes in C_{60}.

there is a single set of symmetrically equivalent atoms and, by symmetry considerations, the normal modes are expected to be completely delocalized. In the case of C_{70}, the 10 atoms of the equatorial belt do constitute a set of symmetrically equivalent atoms and originate symmetry coordinates that are the major contributors of some of the normal vibrations. It is interesting to note that the E_1' mode calculated at 751 cm^{-1} and that, as discussed above, shows the largest deviation from experiments is actually one of the equatorial vibrations.

The correlation between the C_{60} and C_{70} normal vibrations allows a substantial simplification of the interpretation of the spectrum of the latter. Pictorially, this correlation is represented in Figure 5 and Figure 6 for the infrared and Raman active modes. In some regions of the spectrum the correlation is particularly simple and evident. This is for instance the case for the C_{70} modes originating from the A_g and T_{1u} modes and from $H_g(1)$, $H_g(2)$, $H_g(5)$, $H_g(6)$, $H_g(7)$ modes. In particular, for the T_{1u} modes it is seen that the infrared intensity redistributes differently in the correlated C_{70} vibrations.

The attempt to find a regularity in the whole set of vibrational frequencies of C_{70} can be further pursued classifying the normal
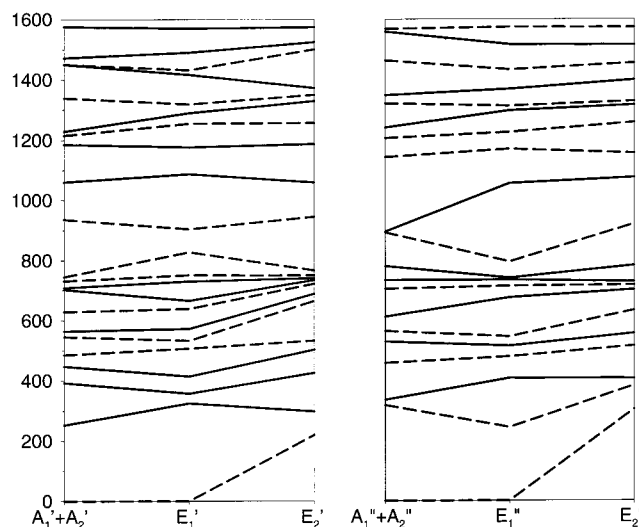
Figure 7. Correlation of the vibrational frequencies of C_{70} according to the cyclic C_5 subgroup. Full and Dotted lines correspond to ν_1 and ν_2 type vibrations.

frequencies of the cluster as originating from a lateral segment of 14 carbon atom under the effect of the rotations of the cyclic C_5 subgroup, as described in the previous section. The dispersion curve type of diagrams obtained is represented in Figure 5, where the correlation for the A_1', A_2', A_1'' and A_2'' modes is shown separately. The diagram has been constructed simply assuming a type of noncrossing rule. The diagram shows how the vibrational frequencies can be correlated in groups of vibrations that only differ in the phase of atomic displacements in different sectors of the cage. Alternatively the diagram is a simpler way of tabulating the vibrational frequencies of the carbon cluster. Since this point of view essentially reduces the C_{70} vibrations to coupled motions of an independent symmetrically inequivalent set of 5 carbon atoms, it also suggests an approach to derive a possible force field for use in molecular dynamics simulations.

Summary and Conclusion

In the present paper starting from a DFT calculation of the vibrational frequencies and of the infrared and Raman intensities an attempt has been made to interpret the vibrational spectra of crystalline C_{70} leading for the first time to a substantially complete assignment of the vibrational frequencies. It has been shown that the DFT approach using the B3-LYP exchange-correlation functional in conjunction with the 6-31G* basis set is a particularly reliable procedure for this type of systems, confirming the results obtained previously in our and in other laboratories. It has been possible to correlate the infrared and Raman spectra of C_{70} with those of C_{60}, distinguishing the vibrational modes of the equatorial belt from those of the semispherical caps. Within the C_{70} cage a possible symmetry correlation among groups of vibrational modes under effect of the C_5 subgroup of the molecular symmetry group is suggested.

References and Notes

(1) Dresselhaus, M. S.; Dresselhaus, G.; Eklund, P. C. *Science of Fullerenes and Carbon Nanotubes*; Academic Press, Inc.: San Diego, CA, 1996.

(2) Cardini, G.; Bini, R.; Salvi, P. R.; Schettino, V.; Klein, M. L.; Stroegin, R. M.; Brand, L.; Smith, A. B., III *J. Phys. Chem.* **1994**, *98*, 9966.

(3) Bini, R.; Procacci, P.; Salvi, P. R.; Schettino, V. *J. Phys. Chem.* **1993**, *97*, 10580.

(4) Martin, M.; Du, X.; Kwon, J.; Mihaly, L. *Phys. Rev. B* **1994**, *50*, 173.

(5) van Loosdrecht, P. H. M.; van Bentum, P. J. M.; Verhejen, M. A.; Meijer, G. *Chem. Phys. Lett.* **1992**, *198*, 587.

(6) Dong, Z.; Zhou, P.; Holden, J. M.; Eklund, P. C. *Phys. Rev. B* **1993**, *48*, 2861.

(7) Giannozzi, P.; Baroni, S. J. *J. Chem. Phys.* **1994**, *100*, 8537.

(8) Schettino, V.; Salvi, P. R.; Bini, R.; Cardini, G. *J. Chem. Phys.* **1994**, *101*, 11079.

(9) Choi, C. H.; Kertesz, M.; Mihaly, L. J. *J. Phys. Chem. A* **2000**, *104*, 104.

(10) Menéndez, J.; Page, J. B. *Topics in Applied Physics;* Springer-Verlag: New York, 2000; Vol. 76, p 27.

(11) Schettino, V.; Pagliai, M.; Ciabini, L.; Cardini, G. *J. Phys. Chem. A* **2001**, *105*, 11192.

(12) Verheijen, M. A.; Meekes, H.; Meijer, G.; Bennema, P.; Deboer, J. L.; Vansmaalen, S.; Vantendeloo, G.; Amelinckx, S.; Muto, S.; Vanlanduyt, J. *Chem. Phys.* **1992**, *166*, 287.

(13) Maniwa, Y.; Ohi, A.; Mizoguchi, K.; Kume, K.; Kikuchi, K.; Saito, K.; Ikemoto, I.; Suzuki, S.; Achiba, Y. *J. Phys. Soc. Jpn.* **1993**, *62*, 1131.

(14) Raghavachari, K.; Rohlfing, C. M. *J. Phys. Chem.* **1991**, *95*, 5768.

(15) Bakowies, D.; Thiel, W. *Chem. Phys.* **1991**, *151*, 309.

(16) Shinohara, Y.; Saito, R.; Kimura, T.; Dresselhaus, G.; Dresselhaus, M. S. *Chem. Phys. Lett.* **1994**, *227*, 365.

(17) Negri, F.; Orlandi, G.; Zerbetto, F. *J. Am. Chem. Soc.* **1991**, *113*, 6037.

(18) Wang, C. Z.; Chan, C. T.; Ho, K. M. *Phys. Rev. B* **1992**, *46*, 9761.

(19) Negri, F.; Orlandi, G. *J. Phys. B* **1996**, *29*, 5049.

(20) Fanti, M.; Orlandi, G.; Zerbetto, F. *J. Phys. B* **1996**, *29*, 5065.

(21) Jishi, R. A.; Dresselhaus, M. S.; Dresselhaus, G.; Wang, K.-A.; Zhou, P.; Rao, A. M.; Eklund, P. C. *Chem. Phys. Lett.* **1996**, *29*, 5065.

(22) Wang, X. Q.; Wang, C. Z.; Ho, K. M. *Phys. Rev. B* **1995**, *51*, 8656.

(23) Onida, G.; Andreoni, W.; Kohanoff, J.; Parrinello, M. *Chem. Phys. Lett.* **1994**, *219*, 1.

(24) Gervasio, F. L.; Cardini, G.; Salvi, P. R.; Schettino, V. *J. Phys. Chem. A* **1998**, *102*, 2131.

(25) Schettino, V.; Gervasio, F. L.; Cardini, G.; Salvi, P. R. *J. Chem. Phys.* **1999**, *110*, 3241.

(26) Chelli, R.; Cardini, G.; Procacci, P.; Righini, R.; Califano, S.; Albrecht, A. J. *J. Chem. Phys.* **2000**, *113*, 6851.

(27) Stratmann, R. E.; Scuseria, G. E.; Frisch, M. J. *J. Raman Spectrosc.* **1998**, *29*, 483.

(28) Rauhut, G.; Pulay, J. *J. Phys. Chem.* **1995**, *99*, 3093.

(29) Scott, A. P.; Radom, L. J. *J. Phys. Chem.* **1996**, *100*, 16502.

(30) Frisch, M. J.; Trucks, G. W.; Schlegel, H. B.; Scuseria, G. E.; Robb, M. A.; Cheeseman, J. R.; Zakrzewski, V. G.; Montgomery, J. A., Jr.; Stratmann, R. E.; Burant, J. C.; Dapprich, S.; Millam, J. M.; Daniels, A. D.; Kudin, K. N.; Strain, M. C.; Farkas, O.; Tomasi, J.; Barone, V.; Cossi, M.; Cammi, R.; Mennucci, B.; Pomelli, C.; Adamo, C.; Clifford, S.; Ochterski, J.; Petersson, G. A.; Ayala, P. Y.; Cui, Q.; Morokuma, K.; Malick, D. K.; Rabuck, A. D.; Raghavachari, K.; Foresman, J. B.; Cioslowski, J.; Ortiz, J. V.; Stefanov, B. B.; Liu, G.; Liashenko, A.; Piskorz, P.; Komaromi, I.; Gomperts, R.; Martin, R. L.; Fox, D. J.; Keith, T.; Al-Laham, M. A.; Peng, C. Y.; Nanayakkara, A.; Gonzalez, C.; Challacombe, M.; Gill, P. M. W.; Johnson, B.; Chen, W.; Wong, M. W.; Andres, J. L.; Gonzalez, C.; Head-Gordon, M.; Replogle, E. S.; Pople, J. A. *Gaussian 98*, revision A.7; Gaussian, Inc.: Pittsburgh, PA, 1998.

(31) Brockner, W.; Menzel, F. *J. Mol. Struct.* **1996**, *378*, 146.

(32) von Czarnowski, A.; Meiwes-Broer, K. H. *Chem. Phys. Lett.* **1995**, *246*, 321.

(33) Procacci, P.; Berne, B. J. J. *J. Chem. Phys.* **1994**, *101*, 2421.

(34) Procacci, P. Private communications.

(35) Lynch, K.; Tanke, C.; Menzel, F.; Brockner, W.; Scharff, P.; Stumpp, E. *J. Phys. Chem.* **1995**, *99*, 7985.

(36) Bowmar, P.; Hayes, W.; Kurmoo, M.; Pattenden, P. A.; Green, M. A.; Day, P.; Kikuchi, K. *J. Phys. Condens. Matter* **1994**, *6*, 3161.

(37) van Loosdrecht, P. H. M.; Verheijen, M. A.; Meekes, H.; van Bentum, P. J. M.; Meijer, G. *Phys. Rev. B.* **1993**, *47*, 7610.

(38) Meilunas, R.; Chang, R. P. H.; Liu, S.; Jensen, M.; Kappes, M. M. *J. Appl. Phys.* **1991**, *70*, 5128.

(39) Christides, C.; Nikolaev, A. V.; Dennis, T. J. S.; Prassides, K.; Negri, F.; Orlandi, G.; Zerbetto, F. *J. Phys. Chem.* **1993**, *97*, 3641.